Comput. Methods Appl. Mech. Engrg. 200 (2011) 2117–2125

Contents lists available at ScienceDirect

Comput. Methods Appl. Mech. Engrg.

journal homepage: www.elsevier.com/locate/cma

Growth model for cholesterol accumulation in the wall of a simplified 3D geometry of the carotid bifurcation

Valeria C. Gessaghi [a,*], Marcelo A. Raschi [b,1], Debora Y. Tanoni [b], Carlos A. Perazzo [c], Axel E. Larreteguy [b]

[a] Facultad de Ingeniería, Universidad Nacional de La Pampa, Calle 110 Esq. 9, Gral. Pico, 6360 La Pampa, Argentina
[b] Instituto de Tecnología, Facultad de Ingeniería y Ciencias Exactas, Universidad Argentina de la Empresa, Buenos Aires, Argentina
[c] Dto. de Física y Química, Universidad Favaloro and CONICET, Buenos Aires, Argentina

ARTICLE INFO

Article history:
Received 4 August 2010
Received in revised form 18 November 2010
Accepted 1 March 2011
Available online 6 March 2011

Keywords:
Atherosclerosis
Hemodynamics
Cholesterol transport

ABSTRACT

Atherosclerosis is one of the leading causes of death in the first world countries nowadays. It is a vascular disease that affects medium and large size arteries, involving the formation of plaques within the artery wall. These plaques result from the accumulation of fat, cholesterol, cell debris, smooth muscle cells and other cells and substances, and may cause temporary or definitive lack of blood supply to an organ.

This article proposes a model for cholesterol accumulation and plaque growth. The model is basically a mass balance of low density lipoproteins (LDL) in the intima. The inflow, outflow, oxidation, and consumption of LDL is modeled combining partial models and correlations available in the literature.

The model was implemented into an open source finite volume code. Assuming steady blood flow, the code was used to predict lesion formation on a three-dimensional model of the carotid artery bifurcation, a location greatly studied for its role in supplying blood to some parts of the brain and for being related to strokes due to formation of atheromas. The simulation was carried out under physiologic conditions for blood pressure and LDL blood concentration.

Results for LDL mass accumulation and intimal thickening over time, plaque shape, and location of thicker spots are reported, showing that the proposed model approximates reasonably well the intimal thickening obtained from post-mortem aortic fatty streaks and from B-mode ultrasonography of the carotid artery of healthy subjects reported by other authors.

1. Introduction

Atherosclerosis is an inflammatory disease that affects large and medium-sized arteries [1]. The atherosclerotic lesion, called *atheroma*, is a focal thickening of the innermost layer of the artery wall, or *intima*. These lesions consist mainly of accumulation of lipids, endothelial and vascular smooth muscle cells (SMC), connective tissue and debris [2]. Atheromas may cause a temporary or permanent lack of blood supply to some organ and is the leading cause of death in developed countries [3]. This is the reason why there has been a big effort devoted to learn and understand its genesis and to find the main risk factors for this disease [4,5].

Atheromas usually develop in arterial bifurcations or regions with marked curvature. Four decades ago, it was proposed that forces exerted by the blood flow on the artery wall have a major influence on the location where these lesions appear [6,7]. Nowadays, researchers agree that atheromas develop in areas with complex flow patterns, such as recirculation and/or secondary flows, where the endothelium is subjected to low and oscillating shear stresses, which are thought to be the cause of the location of the plaques [8,9]. It has been proposed that these low and oscillating stresses may alter the permeability of the endothelium [10,11], favoring extracellular low density lipoproteins (LDL) accumulation and progressive oxidation in these locations. As a consequence, much effort has been done to simulate pulsatile blood flow in these vascular regions to obtain more accurate solutions for each specific patient, while improving the available solution methods [12–14].

Another important event in the initiation of the atheroma is leukocyte recruitment. Monocytes and T lymphocytes tend to accumulate in the early atherosclerotic lesion. The monocytes become macrophages in the artery wall and ingest the oxidized LDL (LDLox) turning into foam cells, commonly found in atheromas [15]. The evolution of the atheroma into a more complex lesion involves SMC migration and proliferation as well as accumulation of other molecules and substances. It is the extracellular matrix rather than the cells themselves that makes up much of the volume of an advanced atherosclerotic plaque, through the accumulation of extracellular matrix macromolecules, such as collagen and proteoglycans produced by the SMCs [15].

* Corresponding author. Tel./fax: +54 2302 422780.
E-mail address: gessaghi@ing.unlpam.edu.ar (V.C. Gessaghi).
[1] Present address: Department of Computational and Data Sciences, College of Science, George Mason University, USA.

0045-7825/$ - see front matter © 2011 Elsevier B.V. All rights reserved.
doi:10.1016/j.cma.2011.03.001

Nomenclature

A	lumen-intima interphase area
BC	boundary conditions
BL	boundary layer
C	concentration of LDL within the intima
C_{bl}	bulk concentration of LDL in blood
C_w	LDL concentration at the lumen-wall interphase
ΔC	transendothelial LDL concentration difference
$\overline{C}_e$	mean endothelial concentration
CCA	common carotid artery
D_{bl}	diffusion coefficient for LDL in blood
D_m	diffusion coefficient for LDL in the media
EC	external carotid artery
e	intimal thickness
FD	flow divider
FVM	finite volume method
IC	internal carotid artery
IEL	internal elastic lamina
J_{in}	total flux of LDL going into the intima
J_{out}	total flux of LDL going out of the intima
J_{diff}	diffusive flux of LDL going out of the intima
J_{conv}	convective flux of LDL going out of the intima
k	reaction rate of LDL oxidation
LDL	Low density lipoprotein
LDLox	oxidized LDL
L_p	endothelial hydraulic conductivity
m	mass of LDL within the intima per unit area
m_{asymp}	asymptotic solution for m
m_{ox}	mass of LDLox within the intima per unit area
$\dot{m}_{cons}$	physiologic rate of consumption of LDL per unit area in the intima
n	simulation time step
p_{bl}	blood pressure
P_d	endothelial diffusive permeability
P_{d0}	scaling constant
p	sub endothelial hydrodynamic pressure
Δp	transendothelial hydrodynamic pressure difference
$\Delta\pi$	trans membrane osmotic pressure difference
$\vec{r}$	position vector
t^n	time at time step n
Δt	time step interval
v_f	plasma filtration velocity
V	total volume of the intima
V_{pl}	volume of the intima occupied by plasma

Greek symbols

α	parameter resulting from the shell mass balance
β	constant in the intimal growth rate equation
γ	parameter resulting from the shell mass balance
δ	hydrodynamic boundary layer thickness
δr	distance from IEL to boundary
μ_∞	Casson asymptotic dynamic viscosity
ρ_{LDL}	density of LDL
ρ_{LDLox}	density of LDLox
σ_e	endothelial reflection coefficient
σ	osmotic intimal reflection coefficient
ϕ	porosity of the intima
τ_y	Casson yield stress

Despite all these processes that occur, some researchers believe that the oxidation of the accumulated LDL is the factor that initiates plaque formation [16]. This is why, lately, some researchers simulated coupled transport of LDL both in the lumen and through the artery wall [17,18]. These works intended to predict the variation of the transendothelial LDL flux along the axial direction of an artery with stenosis, as well as the LDL concentration in the wall. Most of them modeled blood as a Newtonian fluid although it is well known that its non-Newtonian character is relevant in many situations [19]. While a Newtonian model is suitable for simulating flows in regions with high shear rates, non-Newtonian models such as Casson or Carreau–Yasuda give better approximations in regions with low ones [20,21]. As lesions usually develop in areas with low shear rates [22], the use of a non-Newtonian model seems to be the right choice.

In the past few years some researchers tried to build mathematical models of the plaque initiation and growth. Some concentrated on modeling the mechanism of the inflammatory response to study the dynamic behavior of the lesion [23,24] or focusing on the localization of the different molecules within the lesion to study the cap formation [25]. However, none of these works allows the boundary to move nor they account for the spatial variation of the endothelial permeability. In this regard, Gessaghi et al. [26] proposed a model of accumulation of LDL, not including the inflammatory response, but including the spatial variation of the permeability through its dependence of the wall shear stress; and used it to predict initial intimal growth rate focusing on the effect of arterial geometry but with no actual movement of the boundary. Later Calvez et al. [27] proposed a model which predicts the intimal growth rate allowing for the boundary to move in 1-D and 2-D idealized geometries, they also include the spatial variation of the permeability through a cut-off function of the wall shear stress for the 1-D geometry and a Hill function for the 2-D geometry.

We present here a model for predicting plaque initiation and growth due to accumulation of oxidized LDL and other non fat substances within the artery wall. From the works mentioned in the previous paragraphs it is clear that plaque formation is a complex phenomenon, influenced by a variety of factors and there are a few complete mathematical models of the process. However, this work focuses on answering the following question: may a relatively simple model which requires not much computational effort be able to give qualitatively correct predictions of plaque formation and growth? To help answering this question, this model intended to capture the spatial dependence of the phenomena through the dependence of the endothelial permeability on the wall shear stress distribution and was implemented and tested in an idealized three dimensional geometry of the carotid bifurcation.

The rest of the paper is organized as follows. The process for solving this type of problems is described in the next section. In Section 3 the model itself is explained in detail and its application to the idealized carotid bifurcation is described in Section 4, and the corresponding results are presented in Section 5. The discussion of these results is made in Section 6 and in Section 7 the final conclusions are shown.

2. The solution process

Solving a complete growth problem with the proposed model requires a transient simulation which involves performing, for each time step, the stages shown in Fig. 1 and described below.

The first stage consists in the simulation of blood flow inside the flow domain (i.e. an artery), done by solving either analytically or

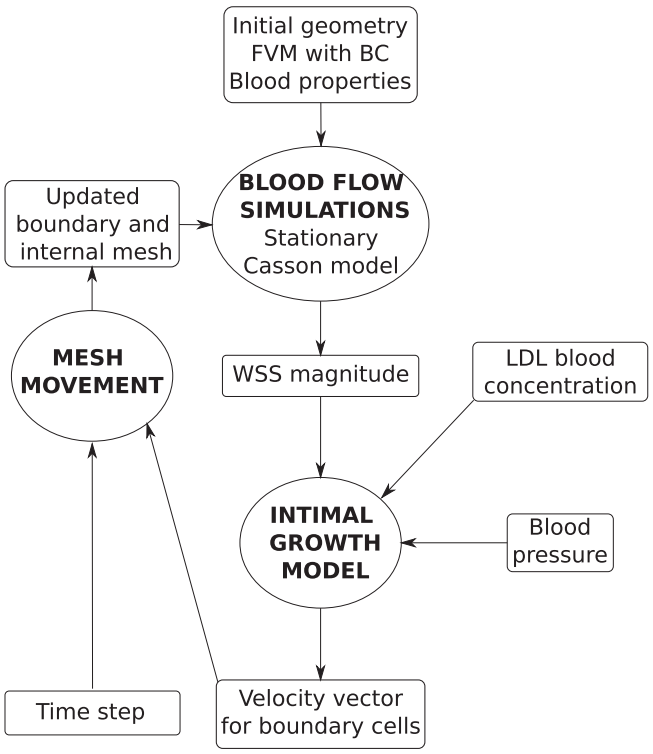

Fig. 1. Block diagram of the stages involved in the process indicating the input parameters and output variables involved in each stage. FVM, finite volume method; BC, boundary conditions.

numerically the corresponding continuity and momentum equations. The flow is assumed steady, since the correlations used for the endothelial transport coefficients do not include dynamic variations of wall shear stresses or any other parameter, making it pointless to use more realistic pulsatile flow simulations. Although the steady state assumption is made here as a first approximation, we are aware that when endothelial permeability is coupled to wall shear stress there are differences between the steady wall shear stresses and the time-averaged unsteady results [28]. Despite it was found up to 30% difference for oxygen transport within the recirculation area, it is also true that this difference is lower for species with high Schmidt number, and Sc for LDL in blood is two orders of magnitude higher than for oxygen [29]. We therefore expect that there is going to be some differences in the wall shear stress distribution obtained but we think that although it may affect the local intimal growth it will not significantly affect the average intimal growth tendency after some iterations.

With the field velocity obtained in this stage we calculate the wall shear stresses in the endothelium, a necessary input for evaluating the endothelial permeability, assumed in our model to depend on them.

The second stage, namely the *intimal growth model*, consists of predicting plaque growth and intimal thickening, modeled as a function of the accumulation of oxidized LDL and other non fat substances in the intima.

The final stage involves using the rate of intimal thickening given by the previous stage and an assumed time step to calculate the new, remodeled, geometry of the artery.

The whole process is repeated time step after time step until a desired final simulation time is reached.

From the point of view of the present model, a problem is completely defined by providing the initial geometry of the domain along with the corresponding flow boundary conditions, the flow properties of blood, the LDL concentration in the blood, and a mean arterial pressure. A reference value for shear stress is also needed, for reasons that will be explained later.

3. The intimal growth model

3.1. The system of equations

The model comprises two main variables that depend on space and time, namely the intimal LDL mass accumulation per unit surface area, $m(\vec{r},t)$, and the intimal thickness, $e(\vec{r},t)$, where $\vec{r}$ represents positions on the endothelium.

For each point $\vec{r}$ on the endothelium, the time evolution $m(\vec{r},t)$ and $e(\vec{r},t)$ result from solving the following coupled first order ordinary differential equations:

$$\dot{m} = \alpha\frac{m}{e} - k\,m + \gamma, \tag{1}$$

$$\dot{e} = \beta\frac{k}{\rho_{LDLox}}m, \tag{2}$$

where k is a constant and where the parameters $\alpha(\vec{r},t)$ and $\gamma(\vec{r},t)$ are functions of the physiologic transport properties of the endothelium, the intima, the media and the physiologic consumption of the intimal cells.

Before engaging in the details of the derivation of each of these two equations, explained in the next two sections, it is important to note the following.

For typical constant values of e, k, α and γ, it results that e evolves very slowly, increasing less than 2% in a one year period. This allows for the assumption that e is approximately constant and consequently there exists an analytical solution for Eq. (1) that is

$$m = \frac{\gamma}{k-\frac{\alpha}{e}} + m_0 e^{(\frac{\alpha}{e}-k)t}, \tag{3}$$

where m_0 is mass of LDL per unit area present in the intima at the initial time. This solution shows a transient behavior with a time constant given by $\frac{1}{\frac{\alpha}{e}-k}$. This value is actually negative and of the order of hours, which leaves us with an asymptotic solution for times longer than a few hours:

$$m_{asymp} = \frac{\gamma}{k-\frac{\alpha}{e}}. \tag{4}$$

Since the time step shown in Fig. 1 was selected to be months or even one year, it is a good approximation to get rid of Eq. (1) and simply replace m_{asymp} into Eq. (2) to predict the growth rate of intimal thickness.

3.2. Equation for LDL mass accumulation

Eq. (1) results from a mass balance, as described below.

The rate of change of the mass of LDL per unit area inside the intima is calculated as (see Fig. 2):

$$\dot{m} = J_{in} - J_{out} - \dot{m}_{ox} - \dot{m}_{cons}, \tag{5}$$

where J_{in} and J_{out} are the fluxes of LDL entering and leaving the intima respectively, and $\dot{m}_{ox}$ and $\dot{m}_{cons}$ are the rates of consumption of LDL by oxidation and by physiologic ingestion of the wall cells per unit area, respectively. All other reactions are neglected and all the fluxes through the arterial wall are assumed to occur only in the radial direction.

3.2.1. Inflow

The first term, J_{in}, is evaluated as follows. The flux of LDL goes through the endothelium and into the intima by two different known pathways, one being the vesicular transport and the other

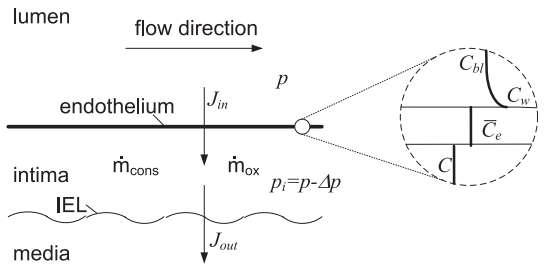

Fig. 2. Schematic illustration of the intimal growth model; the circle on the right shows a closer look at endothelium indicating LDL concentrations at every location. IEL, internal elastic lamina; J_{in} and J_{out}: incoming and outgoing flux of LDL mass, respectively; $\dot{m}_{ox}$ and $\dot{m}_{cons}$: sinks representing the consumption of LDL per unit area and time due to LDL oxidation and due to LDL physiologic ingestion by the wall cells. All other reactions are neglected. All the fluxes through the arterial wall are assumed to occur only in the radial direction.

the transient or leaky junctions. On the other side, the flux of water and other hydrophilic solutes [29,30] have inter cellular junctions as their main pathway. It has been measured, however, that vesicular transport accounts for a scarce 9% of the total LDL transport to the intima [31]. Therefore, we model solute plasma transendothelial transport, following [18,32,33], by means of the Kedem–Katchalsky equations:

$$J_{in} = P_d \Delta C + (1-\sigma_e)\ v_f\ \overline{C}_e, \tag{6}$$

$$v_f = L_p(\Delta p - \sigma_e \Delta\pi), \tag{7}$$

where v_f is the filtration velocity; L_p, P_d and σ_e are the transport parameters of the endothelial membrane regulating plasma and LDL flux into the intima. Defining C and C_w as the LDL concentration within the intima and at the lumen-wall interphase respectively, ΔC, Δp and $\overline{C}_e$ are defined as:

$$\Delta C = C_w - C, \tag{8}$$

$$\Delta p = p_{bl} - p, \tag{9}$$

$$\overline{C}_e = \frac{C_w + C}{2} \approx \frac{C_w}{2}. \tag{10}$$

where p_{bl} and p are the blood and sub endothelial hydrodynamic pressures respectively, and its difference was assumed constant (see Table 1).

To estimate C_w it is used a simple one-dimensional model that balances convective and diffusive transport within the boundary layer (BL), assuming a uniform known concentration outside the BL and a uniform blood pressure. This estimation is valid because there are no reactions occurring in the lumen that can cause LDL to appear or disappear, and because the mass transport BL on the lumen side is very thin compared to the velocity boundary layer (see [29]). This assumptions lead to an exponential solution for the radial distribution of the LDL concentration in the BL. When solving explicitly for C_w it results:

$$C_w \approx C_{bl} e^{\frac{L_p}{D_{bl}}\Delta p \delta}, \tag{11}$$

where D_{bl} is the diffusion coefficient for LDL in blood and δ is the hydrodynamic BL thickness assumed constant based on the Graetz–Nusselt solution for a cylinder of smooth rigid walls with dimensions similar to the common carotid artery [17] (see Table 1).

Eqs. (6) and (7) reflect that the factors that control LDL and water flux across the endothelium are the trans membrane hydrodynamic and osmotic pressure differences and the LDL concentration difference. The osmotic pressure difference $\Delta\pi$ is caused by the presence of many different molecules in the plasma, namely salts, proteins, lipoproteins, etc. The total osmotic pressure difference between plasma and interstitial fluids in the capillaries at body temperature was assumed constant as suggested by others [29,34] (see Table 1).

While L_p and σ_e were assumed constant in the present work (see Table 1), the endothelial diffusive permeability P_d is modeled as a function of the wall shear stress τ_w, as said in the previous section. Although it is not clear how endothelial cells sense τ_w, there are a few empirical models in literature that correlate permeability to macromolecules with different hemodynamic parameters [11,35–37]. Following Himburg et al. [11], the shear-dependent permeability is modeled as:

$$P_d = P_{d0} |\tau_w|^{-0.11}, \tag{12}$$

where P_{d0} is constant scaled so that the permeability is 2×10^{-10} m s^{-1} in the straight portions of the artery, which is considered a normal or reference value in the literature (see Table 1).

3.2.2. Outflow

The second term of Eq. (5), J_{out}, was calculated as the sum of a diffusive and a convective flux, J_{diff} and J_{conv}, defined as:

$$J_{diff} = -D_m \frac{\partial C}{\partial r} \approx D_m \frac{C}{\delta r}, \tag{13}$$

$$J_{conv} = v_f (1-\sigma)\ C, \tag{14}$$

where the D_m and σ were assumed constant (see Table 1). Back in 2005, Prosi et al. [38] showed that both the value and the gradient of LDL concentration within the intima are not sensible to the conditions assumed at the media. In the present model, we assumed that the concentration in the media is negligible at a distance δr from the intima-media interphase, and thus J_{conv} is simply evaluated as proportional to v_f and C.

3.2.3. Oxidation

The third term of Eq. (5), $\dot{m}_{ox}$, is evaluated assuming that all LDL that undergoes oxidation accumulates in the intima, and that this process is an irreversible first order reaction, where the concentration of oxidative agents is much larger than the concentration of LDL. This means that $\dot{m}_{ox}$ results proportional to the mass of LDL per unit area in the intima, m:

$$\dot{m}_{ox} = k\ m, \tag{15}$$

where k is the oxidation rate.

3.2.4. Consumption

The last term, $\dot{m}_{cons}$, represents a sink due to physiologic LDL consumption by the wall cells. Not surprisingly, the results

Table 1
Parameter values used in the model.

Parameter	Value	References
τ_y	0.00864 Pa	[40][a]
μ_∞	0.42 cP	[40][a]
ρ_{bl}	1050 kg/m^3	[41]
ρ_{LDL}	1006–1063 kg/m^3	[41]
k	1.4×10^{-4} s^{-1}	[42]
L_p	3×10^{-12} m s^{-1} Pa^{-1}	[18,32]
σ^e	0.9979	[18,32]
Δp	70 mm Hg	[32][b]
δ	0.012 mm	[17][c]
$\Delta\pi$	25 mm Hg	[43][b]
C_{bl}	1.2 mg/ml	[43][b]
P_{d0}	1.15×10^{-11} Pa$^{0.11}$ ms^{-1}	[38]
D_m	5×10^{-14} m^2/s	[38,32]
D_{bl}	5×10^{-12} m^2/s	[44]
σ	0.8272	[38,32]
ϕ	0.96	[33]
δr	0.1 mm	[38]

[a] Coefficients values for an hematocrite of 47%.
[b] Physiologic values.
[c] Based on Graez–Nusselt solution for a cylinder.

obtained with the model without this sink would predict accumulation of LDL even in regions where it is unlikely to occur under physiologic conditions, i.e., in the straight portions of the arteries. To tackle this problem in a simple manner, the physiologic cell consumption is adjusted in each particular problem to be:

$$\dot{m}_{cons} = (J_{in} - J_{out})|_{reference}, \tag{16}$$

where the *reference* conditions correspond to the physiologic conditions for Δp and C_{bl} (see Table 1), and to a value of τ_w corresponding to straight zones of the flow domain in which there is experimental evidence that there is no significant growth under normal physiologic conditions. For example, straight portions of the carotid artery have values of τ_w higher than 0.5 Pa. It is important to note, however, that this particular value may be more general than simply an example value, because it is also cited by other authors as a threshold value, since lower wall shear stresses are associated with reduction in several vascular wall functions such as endothelial nitric oxide syntheses production, vasodilatation and endothelial cell repair [39].

3.2.5. Closure

Finally, to close the balance it is necessary to eliminate the unknown LDL concentration in the intima, C, by relating it to m and e. Consider a portion of volume V of the intima, defined by a patch of area A and the full thickness e of the intima, so that $V \approx e\,A$. Assuming the intima as a porous medium filled completely with plasma, the volume of the intima effectively occupied by plasma can be expressed as $V_{pl} = V\phi$, where ϕ is the porosity of the intima, assumed constant. Recalling that m is defined as LDL mass per unit area, the concentration may then be expressed as $C = m\ A/V_{pl}$, which for small e results finally in:

$$C = \frac{m}{e\phi}. \tag{17}$$

With all these assumptions Eq. (5) can be rewritten as Eq. (1), where

$$\alpha = \left[\frac{(1-\sigma_e)}{2} - (1-\sigma)\right]\frac{v_f}{\phi} - \left(P_d + \frac{D_m}{\delta r}\right)\frac{1}{\phi}, \tag{18}$$

$$\gamma = \left(P_d + \frac{(1-\sigma_e)}{2}v_f\right)\ C_w - \dot{m}_{cons}. \tag{19}$$

It should be noted that all the parameters in the model are constant in space and time, except for the endothelial permeability that for a given time varies with space through is dependence on the wall shear stress distribution, which in turn varies also in time following the changes in the flow pattern due to remodeling of the arterial geometry. As a consequence, the rate of LDL mass accumulation varies both in space and in time.

Table 1 shows the values adopted in the model for all the parameters, together with the reference to the literature where the value was taken from. It is important to note that although the model developed in this work is valid for lesions on its early stages, based on the conventional histological classification [45], since in more advanced stages other processes such as inflammation and plaque rupture become relevant, there is no exact measure in time of when these stages ends and the lesion evolves to the next one.

3.3. Intimal thickness equation

The rate of change of the intimal thickness or intimal growth rate $\dot{e}$ is modeled as proportional to the rate of accumulation of LDLox mass per unit of lumen–intima interphase area $\dot{m}_{ox}$, as expressed in the following equation:

$$\dot{e} = \beta\frac{1}{\rho_{LDLox}}\dot{m}_{ox}. \tag{20}$$

By simply substituting $\dot{m}_{ox}$ using Eq. (15) we get the final expression, Eq. (2).

Four major assumptions are made here, the first two being that LDLox concentration relates to LDLox volume through the LDLox density, and that the densities of LDL and LDLox are equal. These assumptions are based on the fact that in early lesions lipoprotein particles appear to decorate the proteoglycan of the arterial intima, abandoning the solution state and coalescing into aggregates bounded to the extracellular matrix, having increased susceptibility to oxidative or other chemical modifications [15].

The third assumption is that the concentration of LDLox within the intima remains fixed and constant, with the consequence that changes in LDLox mass would lead directly to a corresponding change of intimal volume.

Finally, the fourth assumption is that local relative changes in interphase area are negligible compared to local relative changes in thickness.

Constant β is intended to consider the contribution of additional accumulation of non-lipidic substances. A study made by Guyton [43] found that in lesions obtained from people that died from causes other than atherosclerosis, approximately 50% of the total intimal thickening of post-mortem human aortic fatty streaks was due to lipid accumulation and the rest to collagen and other non-lipidic substances. We set then $\beta = 2$ to account for this additional non-lipidic accumulation. It is important to note that it was also assumed that the intima grows always toward the lumen side, therefore reducing the arterial lumen cross-section.

4. Application to a simplified carotid

The model has been applied to a simplified carotid bifurcation. The relevance of this artery comes from the fact that it supplies blood to the brain and that it is prone to develop atheromas in its bifurcation, which may cause stroke.

4.1. Implementation

The whole solution process was implemented into OpenFOAM v1.4.1 [46], a set of libraries for developing applications involving field operations and manipulations. OpenFoam uses finite volume techniques to transform differential equations into algebraic approximations.

The blood flow solver is basically *simpleFoam*, a freely available application based on OpenFOAM for simulating steady incompressible flows, which relays in the renowned SIMPLE algorithm [47] to solve for the pressure and velocity fields. In order to solve for the flow, a three-dimensional flow mesh composed of polyhedral finite volumes must be constructed for discretizing the domain of interest.

For simulating the intima, a one-layer three-dimensional *growth mesh* was defined, coincident with the surface elements of the *flow mesh*. The growth model predicts discrete growth velocities for each node of this surface (growth) mesh.

The dynamic motion solver (DMS) already available in OpenFoam was used to update the geometry and its corresponding finite volume mesh in each time step. The DMS moves the surface mesh nodes based on a velocity provided (in this case the intimal thickness growth rate) and accommodates the rest of the mesh using a Laplacian transformation.

Blood is assumed as a homogeneous, non-Newtonian fluid, modeled using the Casson equation previously studied and used by others [19,48,49], with the coefficients shown in Table 1. The Casson model was implemented as a dynamic library in OpenFoam and validated for a benchmark case of steady flow in a cylinder. The velocity profile obtained numerically correlated within 5%

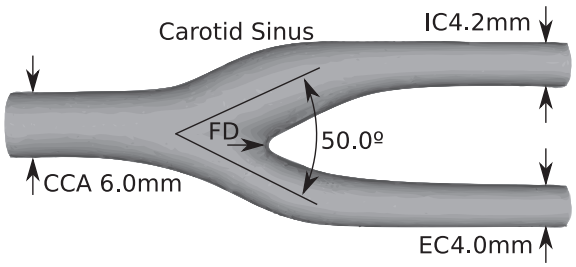

Fig. 3. Carotid bifurcation geometry. Arrows mark inner diameters of common (CCA), external (EC) and internal (IC) carotid arteries and flow divider (FD).

with the theoretical solution, with a 2% error in the calculation of τ_w.

4.2. Description of the case

The geometry corresponds to the simplified carotid bifurcation of reference [50]. Fig. 3 shows the initial domain used for the flow simulations, with some relevant diameters and the so-called flow divider (FD) indicated.

The finite volume flow mesh, generated with Netgen [51], has 484449 tetrahedral elements. The condition of flow is laminar, with $Re_d = 440$, and assumed steady. A parabolic steady profile was used as inlet boundary condition at the common carotid artery (CCA). A stress free condition was used as the outlet boundary condition on the internal carotid and a fixed pressure was used on the external carotid to achieve an exit volumetric flow relation of 70:30 between the internal (IC) and external (EC) carotid arteries. For the flow simulations the wall was assumed rigid and impermeable since the blood flow that permeates the endothelium is many orders of magnitude lower that the arterial flow.

A constant time interval Δt of 6 months was selected for all the simulation. The initial thickness of the intima was given the value $e_i^0 = 50$ μm.

5. Results

Fig. 4 shows three views (anterior, lateral and posterior) of the carotid bifurcation, colored based on e predicted by the model for a 50 years old person who maintained physiologic conditions for the past 30 years. The thickness e varies from 50 μm, which was the initial value, up to 160 μm in the red spots, identified as $P1$, $P2$, $P3$ and $P4$ on the external walls. Since trans membrane hydrodynamic and osmotic pressures were assumed constant, the filtration velocity results 2.4810^{-5}mm/s which is within 7% of the value obtained by Yang et al. [32]. To show more clearly the modification of the wall thickness and the lumen cross-section, Fig. 5 shows two arterial cuts showing the lumen cross-section reduction after 50 years. On the left the horizontal lines show the axial positions where the axial cuts are obtained. On the right there are the initial and final lumen cross-section.

Fig. 6(a) shows the same three views of the bifurcation, now colored based on $|\tau_w|$ distribution. Fig. 6(b) shows $|\tau_w|$ along two lines defined by the intersection of the symmetry planes and the external walls of the bifurcation, as indicated by the black line in the inset at the bottom right corner of the plot. There are locations where τ_w is reduced up to two orders of magnitude from that found in the CCA. The reduced shear stress zone, a consequence of the secondary flows caused by the presence of the bifurcation itself and the effect of the carotid sinus on the IC, begins upstream from the FD, spreading wider in the IC wall than in the EC wall.

To have more quantitative values of e the distribution shown in Fig. 4 was averaged over three regions called IC plaque, EC plaque,

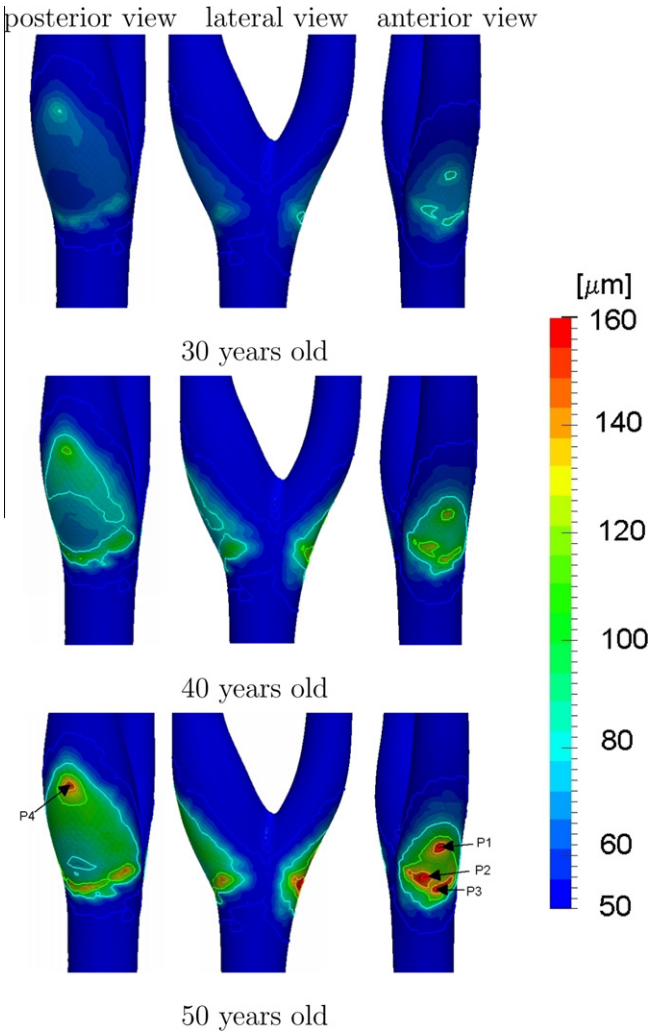

Fig. 4. Color plot and contour lines of intimal thickness at ages of 30, 40 and 50 years old, for a person with blood pressure of 120 mm Hg, $C_{bl} = 1.2$ mg/ml and an initial uniform intimal thickness of 50 μm at age of 20 years old. Contour line colors values are: blue for 50 μm, light blue for 80 μm, green for 110 μm, orange for 140 μm and red for 160 μm. (For interpretation of the references to colour in this figure legend, the reader is referred to the web version of this article.)

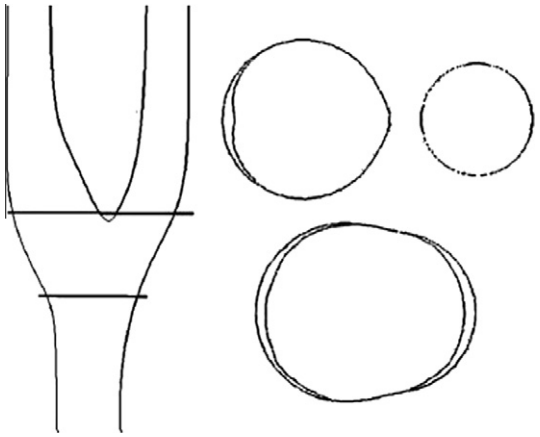

Fig. 5. Lumen cross-section reduction after 50 years. Left: horizontal lines showing the axial positions where the axial cuts are obtained. Right: initial and final lumen cross-section.

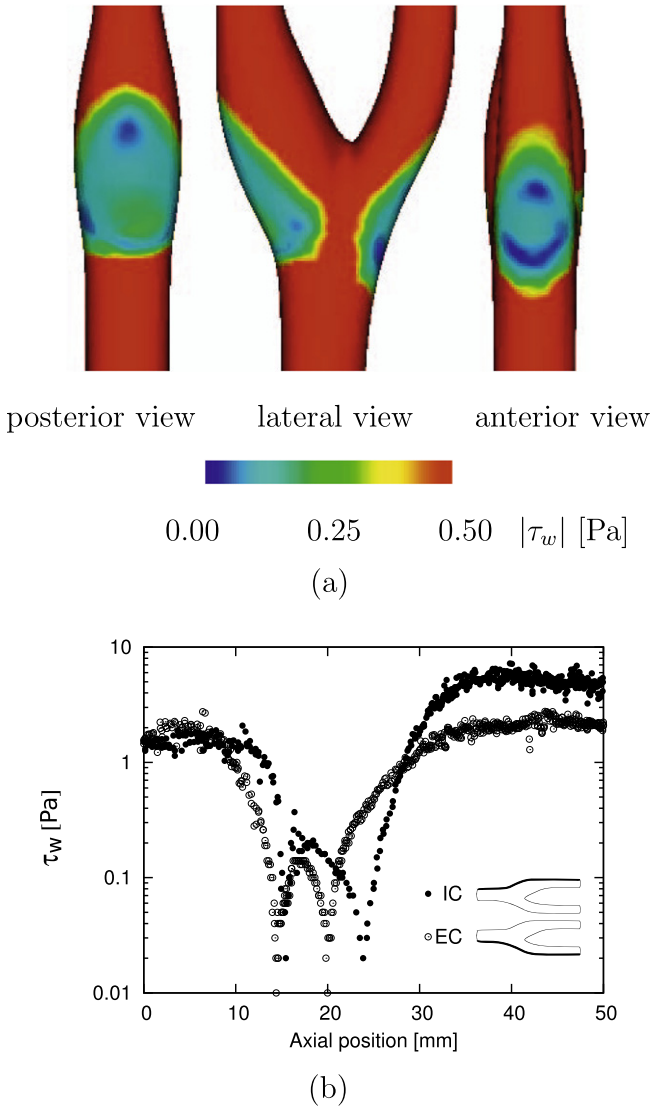

Fig. 6. (a) $|\tau_w|$ distribution in the carotid bifurcation for the initial geometry. (b) $|\tau_w|$ along central lines on the externals walls of the EC and the IC.

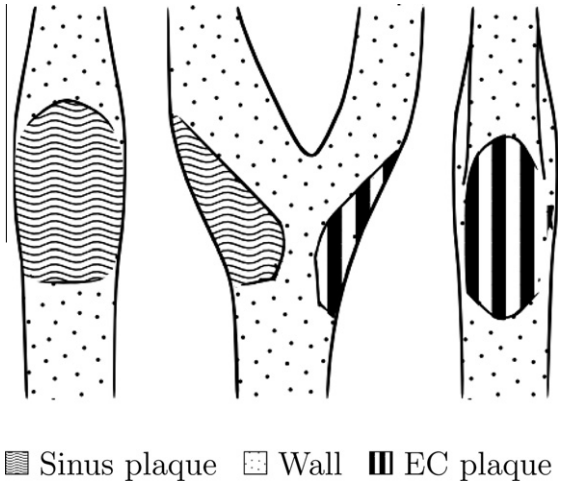

Fig. 7. Integration areas defined to obtain intimal average and local maximum values: IC plaque, EC plaque and wall.

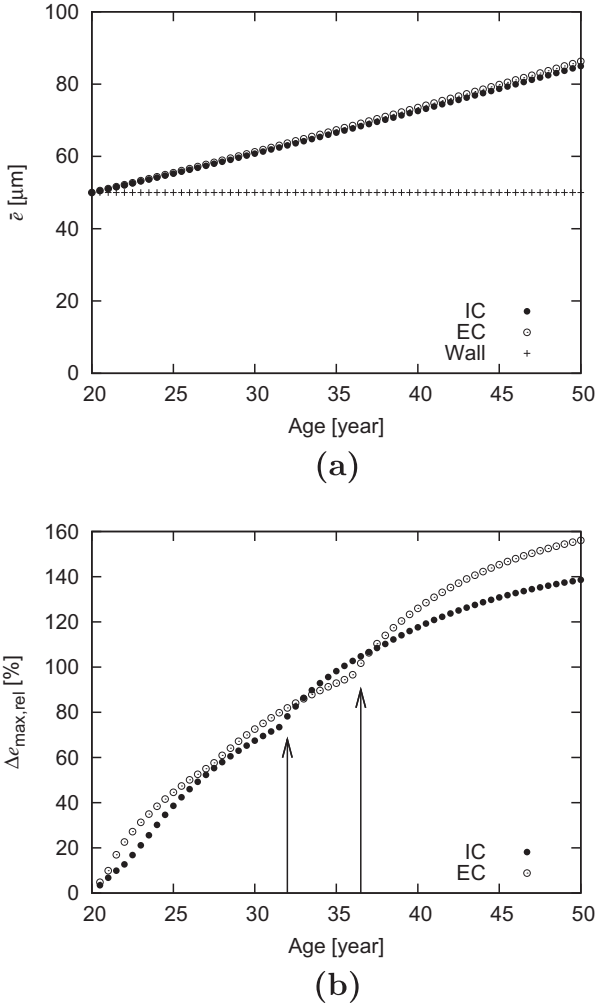

Fig. 8. (a) Average e over time for physiologic conditions, for the IC and EC plaques and for the wall. (b) $\Delta e_{max,rel}$ over time for the IC and EC plaques.

and wall, defined as shown in Fig. 7. Fig. 8(a) shows the time evolution of the average intimal thickness, $\bar{e}$, for physiologic conditions, for the IC and EC plaques, which shows a mostly linear dependence with time. It is also shown for the rest of the arterial surface, where it is clear that there has been no growth at all.

In order to measure the evolution of the thickest spots of the plaque, it is useful to introduce the time dependent magnitude $\Delta e_{max,rel}$, defined as the percent relative difference between the maximum e and the average $\bar{e}$. A value of $\Delta e_{max,rel} = 0$ would indicate that the lesion has no peaks nor valleys, while increasing values indicate increasing the presence of non-uniformity due to privileged growth on selected thick spots. The time evolution of $\Delta e_{max,rel}$ computed for the IC and EC plaques are shown in Fig. 8(b).

Fig. 9(a) shows the *total* mass of LDL accumulated over time within the intima of the IC and EC plaques, with the IC lesion reaching a maximum of 0.023 μgr at the age of 50, and the EC lesion a lower value of 0.015 μgr at the same age.

The same plot, but for LDLox mass, is shown in Fig. 9(b). LDLox mass also shows an approximately linear increase over time, predicting a rate of accumulation of about 92 μgr/year in the IC and of 63 μgr/year in the EC.

6. Discussion

Fig. 4 shows that intimal thickening occurs on the external walls of the bifurcation, indicated by the non blue areas and the contour lines.

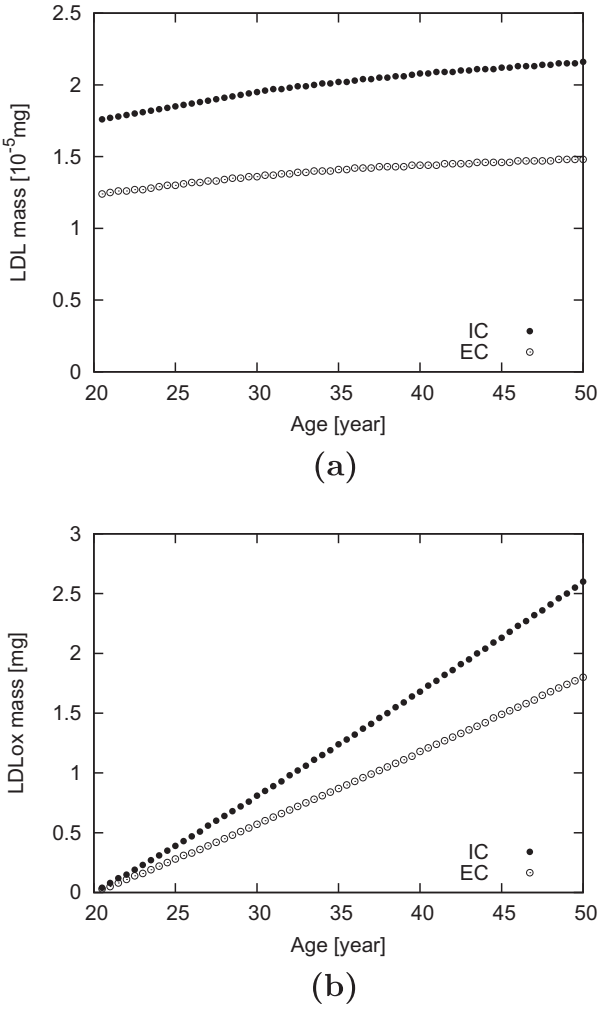

Fig. 9. Cholesterol accumulation in the IC and EC plaques over time for physiologic conditions. (a) LDL mass, (b) LDLox mass.

Comparing Figs. 4 and 6(a), it is evident that the areas where $\tau_w < 0.5$ Pa coincide with the areas where growth has occurred, as expected. Also the areas with thicker e correspond to areas of lower τ_w. This indicates that, for physiologic conditions, the wall shear dependent diffusive flux dominates over the shear independent convective flux. Furthermore, it was previously showed by the authors that the non Newtonian behavior of blood flow seems to have an athero-protective effect because although the distribution of the wall shear stress is similar in both cases, the points of lowest value are lower for the Newtonian than for the non Newtonian behavior, causing the initial growth rate of the wall to be relatively higher for the former [52].

Fig. 8(a) shows that for the simulated conditions, after 20 years, at an age of about 40, the e of the IC and EC lesions has increased to 72 μm, a 45% increase from the initial value. Guyton [43] measured an intimal thickening of 40% in post-mortem human aortic fatty streaks of people between 25 and 45 years old. Also Homma et al. [53] measured the CCA intima-media thickness of 319 healthy subjects using B–Mode Ultrasonography, whose age ranged between 21 to 105 years. They found a linear tendency that resulted in a thickening rate of 9 μm/year ($r = 0.83$). In our simulations, we observed an average intimal thickening of about 1.3 μm/year at the carotid sinus and of 5 microns/year at local maximum, values of the same order of magnitude of that obtained by Homma et al. [53].

As described in the previous section, the curve in Fig. 8(b) speaks about height of the peaks of the lesions. Over the first 40 years of the simulation the thick spots tend to grow faster than average increasing the thickness of the thick spots, a tendency that fades out with time indicating that both lesions seem to approach more stable shapes. The whole plaque keeps growing at the same rate, indicated by the fact that the difference remains almost constant. Inflexions in the curves, pointed with arrows, indicate the moments when the absolute maximum changes to a different spot. This movement of the maximum shows that as arterial geometry changes with time so does τ_w distribution and consequently $\dot{e}$. Since τ_w at these locations does not necessarily change linearly with time, $\Delta e_{\max,rel}$ does not follow a linear tendency.

Finally, Fig. 9(a) and (b) show that both LDL and LDLox mass accumulates focally in the IC and EC plaques. LDL mass increases rapidly in the first year and then tends to an almost constant value on both lesions, while the linear increase of the integrated LDLox mass accumulation explains the linear tendency of the average thickness $\bar{e}$.

7. Conclusion

A model for LDL accumulation and intimal thickening has been presented. Plaque growth and intimal thickening is modeled as a function of the accumulation of LDLox in the intima. The model is based on a balance of LDL mass in the intima along with relations for calculating the rate of LDL oxidation and the corresponding rate of increase of the intimal thickness.

The model was applied to a three-dimensional simplified carotid bifurcation geometry. A Finite Volume technique was used for simulating blood flow in the artery, which was in turn used for computing wall shear stresses, assumed by the model to control endothelial permeability. One important result predicted by our model, for the conditions analyzed, is that the average intimal thickness that occurs on the external walls of the carotid bifurcation follows an almost linear relation with time, although locally thick spots do not necessarily follow the same tendency.

The model seems to include the most fundamental processes since it reproduces adequately some qualitative aspects of the phenomenon, namely, that the thickness of the wall increases significantly in a few small areas, and that these areas are located in the exterior walls of the carotid bifurcation.

There is not much quantitative information available to validate our model further. However, comparison with experimental values found by other authors is good, since it predicts growths with the same linear tendency and with a rate of the same order of magnitude.

It should be kept in mind, however, that the predictions of this model are valid for lesions in its early stages, since in more advanced stages other processes not included in the present model, such as inflammation and plaque rupture, become relevant.

In order to plan for future developments, some processes that could be included to have a more realistic idea of the evolution of the early lesions are, for example, macrophage migration and accumulation, changes in endothelial permeability caused by cell apoptosis due to hypoxia, or the effect of high density lipoproteins causing a reverse LDL flow and reducing the LDLox concentration within the intima.

A much more challenging task would be to include in the model factors such as SMC migration and reproduction, inflammatory effects which causes lots of *T*-cells and monocytes to migrate and accumulate, and extracellular matrix segregation. Modeling advanced lesion stages, not only requires accounting for the accumulation of a great variety of substances but also the modeling of other complex phenomena such as cup erosion or rupture and thrombosis.

The authors believe that this simple model is a starting point to study the influence of different risk factors such as arterial blood pressure and LDL concentration in blood, and to compare their relative influence on the early lesion shape and growth rate.

Acknowledgments

The authors thank the support of Agencia Nacional de Promoción Científica y Tecnológica of Argentina through the Program for Technological Modernization, BID 1728/OC-AR. VCG thanks the support of Facultad de Ingeniería, UNLPam. CAP thanks grants PICTO 21360.

References

[1] R. Ross, Atherosclerosis – an inflammatory disease, N. Engl. J. Med. 340 (1999) 115–126.
[2] J. Berliner, M. Navab, A. Fogelman, J. Frank, L. Demer, P. Edwards, A. Watson, A. Lusis, Atherosclerosis: basic mechanisms: oxidation, inflammation, and genetics, Circulation 91 (1995) 2488–2496.
[3] A.H.A.S. Commitee, S.S. Subcommitee, Heart diseases and stroke statistics – 2007, update at-a-glance. <www.americanheart.org>, 2007.
[4] R. Altman, Risk factors in coronary atherosclerosis athero-inflammation: the meeting point, Thromb. J. 1 (2003) 4.
[5] A. Hinderliter, M. Caughey, Assessing endothelial function as a risk factor for cardiovascular disease, Curr. Atheroscler. Rep. 5 (2003) 506–513.
[6] D. Fry, Certain histological and chemical responses of the vascular interface to acutely induced mechanical stress in the aorta of the dog, Circ. Res. 24 (1969) 93–108.
[7] C. Caro, J. Fitz-Gerald, R. Schroter, Atheroma and arterial wall shear. Observation, correlation and proposal of a shear dependent mass transfer mechanism for atherogenesis, Proc. R. Soc. Lond. B: Biol. Sci. 177 (1971) 109–159.
[8] M. Friedman, D. Giddens, Blood flow in major blood vessels: modeling and experiments, Ann. Biomed. Engrg. 33 (2005) 1710–1713.
[9] D. Ku, Blood flow in arteries, Annu. Rev. Fluid Mech. 29 (1997) 399–434.
[10] O. Ogunrinade, G. Kameya, G. Truskey, Effect of fluid shear stress on the permeability of the arterial endothelium, Ann. Biomed. Engrg. 30 (2002) 430–446.
[11] H. Himburg, D. Grzybowski, A. Hazel, J. LaMack, X.M. Li, M. Friedman, Spatial comparison between wall shear stress measures and porcine arterial endothelial permeability, Heart Circ. Physiol. 286 (2004) H1916–H1922.
[12] I.E. Vignon-Clementel, C.A. Figueroa, K.E. Jansen, C.A. Taylor, Outflow boundary conditions for three-dimensional finite element modeling of blood flow and pressure in arteries, Comput. Methods Appl. Mech. Engrg. 195 (2006) 3776–3796.
[13] P. Blanco, R. Feijóo, S. Urquiza, A unified variational approach for coupling 3d1d models and its blood flow applications, Comput. Methods Appl. Mech. Engrg. 196 (2007) 4391–4410.
[14] H. Kim, C. Figueroa, T. Hughes, K. Jansen, C. Taylor, Augmented lagrangian method for constraining the shape of velocity profiles at outlet boundaries for three-dimensional finite element simulations of blood flow, Comput. Methods Appl. Mech. Engrg. 198 (2009) 3551–3566.
[15] E. Braunwald, D. Ziper, P. Libby, The Vascular Biology of Atherosclerosis, Saunders W.B.C.O, 2001.
[16] J. Holtzman, Atherosclerosis and Oxidant Stress: A New Perspective, Springer-Verlag, New York, 2008.
[17] D. Stangeby, C. Ethier, Computational analysis of coupled blood-wall arterial LDL transport, J. Biomech. Engrg. 124 (2002) 1–8.
[18] N. Sun, N. Wood, A. Hughes, S. Thom, X. Xu, Fluid-wall modelling of mass transfer in an axisymmetric stenosis: effects of shear-dependent transport properties, Ann. Biomed. Engrg. 31 (2006) 1–10.
[19] Y. Fung, Mechanical properties of living tissue, biomechanics, second ed., Springer-Verlag, New York, 1993.
[20] J. Chen, X. Lu, Numerical investigation of the non-Newtonian pulsatile blood flow in a bifurcation model with a non-planar branch, J. Biomech. 39 (2006) 812–832.
[21] F. Basombrio, E. Dari, G. Buscaglia, R. Feijoo, Numerical experiments in complex hemodynamic flows. non-Newtonian effects, Int. J. Comput. Fluid Dyn. 16 (2002) 231–246.
[22] C. Zarins, D. Giddens, B. Bharadvaj, V. Sottiurai, R. Mabon, S. Glagov, Carotid bifurcation atherosclerosis. Quantitative correlation of plaque localization with flow velocity profiles and wall shear stress, Circ. Res. 53 (1983) 502–514.
[23] A.I. Ibragimov, C.J. McNeal, L.R. Ritter, J.R. Walton, A dynamic model of atherogenesis as an inflammatory response, Adv. Dyn. Syst. 14 (2007) 185–189.
[24] A. Ougrinovskaia, R. Thompson, M. Myerscough, An ode model of early stages of atherosclerosis: mechanisms of the inflammatory response, Bull. Math. Biol. 75 (2010) 1534–1561.
[25] A.I. Ibragimov, C.J. McNeal, L.R. Ritter, J.R. Walton, A mathematical model of atherogenesis as an inflammatory response, Math. Med. Biol. 22 (2005) 305–333.
[26] V. Gessaghi, M. Raschi, A. Larreteguy, C. Perazzo, Influence of arterial geometry on a model for growth rate of atheromas, J. Phys. Conf. Ser. 90 (2007) 012046.
[27] V. Calvez, A. Ebde, N. Meunier, A. Raoult, Mathematical modelling of the atherosclerotic plaque formation, Proc. R. Soc. Lond. Ser. B. Biol. Sci. 28 (2009) 1–12.
[28] C. Ethier, Computational modeling of mass transfer and links to atherosclerosis, Ann. Biomed. Engrg. 30 (2002) 461–471.
[29] J. Tarbell, Mass transport in arteries and the localization of atherosclerosis, Ann. Rev. Biomed. Engrg. 5 (2003) 79–118.
[30] C. Michel, F. Curry, Microvascular permeability, Physiol. Rev. 79 (1999) 703–761.
[31] L. Cancel, A. Fitting, J. Tarbell, In vitro study of LDL transport under pressurized(convective) conditions, Am. J. Physiol. Heart Circ. Physiol. 293 (2007) H123–H132.
[32] N. Yang, K. Vafai, Modeling of low-density lipoprotein (LDL) transport in the artery-effects of hypertension, Int. J. Heat Mass Transfer 49 (2006) 850–867.
[33] N. Yang, K. Vafai, Low-density lipoprotein (LDL) transport in an artery – a simplified analytical solution, Int. J. Heat Mass Transfer 51 (2008) 497–505.
[34] L. Hodgson, J. Tarbell, Solute transport to the endothelial intercellular cleft: the effect of wall shear stress, Ann. Biomed. Engrg. 30 (2002) 936–945.
[35] G. Rappitsch, K. Perktold, Computer simulation of convective diffusion processes in large arteries, J. Biomech. 29 (1996) 207–215.
[36] M. Friedman, D. Fry, Arterial permeability dynamics and vascular disease, Atherosclerosis 104 (1993) 189–194.
[37] J. LaMack, H. Himburg, X.M. Li, M. Friedman, Interaction of wall shear stress magnitude and gradient in the prediction of arterial macromolecular permeability, Ann. Biomed. Engrg. 33 (2005) 457–464.
[38] M. Prosi, P. Zunino, K. Perktold, A. Quarteroni, Mathematical and numerical models for transfer of low-density lipoproteins through the arterial walls: a new methodology for the model set up with applications to the study of disturbed lumenal flow, J. Biomech. 38 (2005) 903–917.
[39] K. Cunningham, A. Gotlieb, The role of shear stress in the pathogenesis of atherosclerosis, Lavoratory Invest. 85 (2005) 9–23.
[40] E. Merrill, W. Margetts, G. Cokelet, E. Gilliland, The Casson equation and rheology of blood near zero shear, in: A. Copley (Ed.), Symposium on Biorheology, Interscience Publishers, New York, 1963, pp. 135–143.
[41] A. Blanco, Qufmica biolgica, El Ateneo, Buenos Aires, sexta ed., 1997.
[42] K. Fukuzawa, Y. Inokami, A. Tokumura, J. Terao, A. Suzuki, Rate constants for quenching singlet oxygen and activities for inhibiting lipid peroxidation of carotenoids and α-tocopherol in liposomes, Lipids 33 (1998) 751–756.
[43] J. Guyton, K. Klemp, Transitional features in human atherosclerosis. Intimal thickening, cholesterol clefts, and cell loss in human aortic fatty streaks, Am. J. Pathol. 143 (1993) 1444–1457.
[44] S. Tada, J. Tarbell, Oxygen mass transport in a compliant carotid bifurcation model, Ann. Biomed. Engrg. 34 (2006) 1389–1399.
[45] H. Stary, Natural history and histological classification of atherosclerotic lesions: an update, Arterioscler. Thromb. Vasc. Biol. 20 (2000) 1177–1178.
[46] OpenFoam, The Open Source CFD Toolbox. <www.opencfd.co.uk/openfoam/index.html>, 2007.
[47] S. Patankar, Numerical Heat Transfer and Fluid Flow, Hemisphere Publishing Corporation, 1980.
[48] M. Lei, C. Kleinstreuer, G. Truskey, A focal stress gradient-dependent mass transfer mechanism for atherogenesis in branching arteries, Med. Engrg. Phys. 18 (1996) 326–332.
[49] K. Perktold, M. Resch, H. Florian, Pulsatile non-newtonian flow characteristics in a three-dimensional human carotid bifurcation model, J. Biomech. Engrg. 113 (1991) 464–476.
[50] M. Khakpour, K. Vafai, Critical assessment of arterial transport models, Int. J. Heat Mass Transfer 51 (2008) 807–822.
[51] J. Schoberl, NETGEN – automatic mesh generator. <www.hpfem.jku.at/netgen/>, 2004.
[52] V. Gessaghi, M. Raschi, A. Larreteguy, C. Perazzo, Influencia de las caracterfsticas reolgicas y no estacionarias del flujo sangufneo en un modelo de crecimiento de placas aterosclerticas, Mecnica Comput. XXV (2006) 759–771.
[53] S. Homma, N. Hirose, H. Ishida, T. Ishii, G. Araki, J.H. Halsey, Carotid plaque and intima-media thickness assessed by B-mode ultrasonography in subjects ranging from young adults to centenarians, Stroke 32 (2001) 830–835.